INTERNATIONAL JOURNAL FOR NUMERICAL METHODS IN FLUIDS
Int. J. Numer. Meth. Fluids 2000; **32**: 97–117

Numerical investigation of the aerodynamics of the near-slot film cooling

P.G. Kassimatis[a], G.C. Bergeles[b], T.V. Jones[a] and J.W. Chew[c,*]

[a] *Department of Engineering Science, University of Oxford, Parks Road, Oxford, UK*
[b] *Fluids Section, Department of Mechanical Engineering, National Technical University of Athens, Athens, Greece*
[c] *Department of Mechanical Methods, Technology, Rolls-Royce plc, PO Box 31, Derby, DE24 8BJ, UK*

SUMMARY

Fluid injection from slot or holes into cross-flow produces highly complicated flow fields. Physical situations encountering the above problem range from turbine blade cooling to waste discharge into rivers. In this paper, the flow field created by a two-dimensional slot cooling geometry is examined using the finite volume approach with a second-order upwind differencing scheme. The time-averaged Navier–Stokes equations were solved on a collocated Cartesian grid with a two-equation model of turbulence. Attempting to solve the flow field by assuming a uniform velocity profile at the slot exit leads to inaccurate results, while extending the solution domain improves significantly the results, but proves to be costly, both in memory and in computing time (particularly in the case of multiple holes). A pressure-type boundary condition, based on uniform total pressure, is developed for the slot exit (easily applied to a three-dimensional geometry), which yields more accurate results than the widely used uniform velocity assumption. It is also found that the implementation of low Reynolds number turbulence models on this geometry provides no significant differences from the standard k–ε model.

KEY WORDS: Navier–Stokes equations; two-dimensional slot cooling; film cooling; numerical methods

1. INTRODUCTION

The flow characteristics of a jet in a cross-flow are determined by a large number of parameters, such as velocity ratio, injection angle, exit geometry, Reynolds number, etc. These parameters vary in different engineering situations. To stabilise the flame in a combustion chamber, a large velocity ratio is needed, while for the film cooling of a gas turbine blade much smaller ratios are required. In modern gas turbine engines, higher inlet temperatures are needed to achieve high thrust and power and to reduce fuel consumption. Blade cooling through surface slots or holes (along with internal cooling) allows considerably higher inlet gas

* Correspondence to: Department of Mechanical Methods, Technology, Rolls-Royce plc, PO Box 31, Derby, DE24 8BJ, UK.

CCC 0271–2091/2000/010097–21$17.50

Received July 1996
Revised September 1996

temperatures than the blade could otherwise withstand. Thus, an optimisation problem arises, since a low cold stream flux can lead to insufficient cooling, while a high cold stream flux can reduce the overall temperature, and therefore can reduce the thermal efficiency. Furthermore, any increase in the size or the number of the slots may affect the structural integrity of the blade.

A theoretical model was proposed by Fitt *et al.* [1] for a normal slot geometry trying to quantify the effect on the flow within a slot due to the main/secondary fluid interaction. The model assumed no separation at the slot trailing edge, and viscous effects were neglected. The predicted mass flow characteristic was in close agreement with the experiment at injection rates high enough to have unimportant viscous interactions, and sufficiently low to avoid large separations. One important aspect of this theory is the 'lid effect': separation from the front of the slot is tangential to the wall, and the mainstream acts as a lid over the slot forcing all the injected fluid to emerge from a region close to the rear vertex. Thus, the mass flow of the injectant is reduced, weakening the cooling effect as well. In order to avoid this effect, Fitt and Wilmott [2] suggested a forced non-zero angle of separation by modifying the geometry of the problem (stepped slot with an artificial ramp at the upstream end).

Since the literature on experimental research on film cooling covers a wide range, the work most relevant to this paper will be briefly mentioned. In research conducted at Oxford, O'Malley [3] and Fitt *et al.* [1] produced experimental data for a 90° slot for different blowing ratios. The flow considered was isothermal and the aerodynamics of slot cooling was investigated. Bergeles *et al.* [4] investigated the character of a normal jet discharged into a main stream through a hole. Measurements at the jet exit showed that strong variations of static pressure around the hole produce a substantially non-uniform velocity profile at the jet exit. The same authors [5] examined the case of a jet inclined at 30° discharging into the main flow. Below a certain injection ratio, the injectant remains essentially attached to the surface, again producing strong surface pressure distortions; above this ratio, the jet lifts off the surface allowing penetration of the main stream fluid beneath. In contrast to a 90° slot, appreciable disturbances to the flow field mainly affect the region downstream of the hole. Similar conclusions have been reported by Andreopoulos [6]. The film cooling effect of a slot geometry has also been investigated. Bergeles *et al.* [4] presented data for local cooling effectiveness demonstrating the need for injection rate optimisation in discrete hole geometries. Metzger *et al.* [7] produced results for two-dimensional cooling by non-tangential injection slots, varying the angle of injection. Teekaram *et al.* [8] investigated the case for subsonic injection from a 30° slot into a flow that accelerated to supersonic conditions.

In this paper, a numerical solution of the time-averaged Navier–Stokes equations for a two-dimensional normal slot geometry is examined and compared with experimental data. Emphasis is given to the fluid behaviour inside the slot, to better explain the physical basis of the near-slot region and to obtain a more realistic boundary condition than the one commonly used. This will enable a better approximation in cases where the slots cannot be efficiently resolved, as in the case of a modern turbine blade, which includes numerous slots. This attempt was initiated by the large differences in results of the resolved and the unresolved slot case, and the observation that, in a range of injection ratios, the stagnation pressure profile is uniform. For one injection ratio, three low Reynolds number turbulence models were used along with the curvature modification of the $k-\varepsilon$ model to test their suitability in this geometry. Briefly,

the main topics in this paper are as follows: a description of the numerical methodology, a presentation of computational results compared with the experimental data, turbulence models examined in this geometry, a discussion of the flow field in the vicinity of the slot and testing of the slot exit boundary conditions.

2. NUMERICAL METHOD

The numerical results presented in this paper have been obtained using the Reynolds equations describing the turbulent motion of the gas flow. The time-averaged form of continuity, momentum and conversation equations for scalar variables were numerically solved using a collocated grid with Cartesian velocity components. Turbulence was simulated by the two-equation $k-\varepsilon$ model with wall functions. Three low Reynolds number versions of the $k-\varepsilon$ model were also used to test their suitability on a slot geometry. Discretisation was based on the finite volume approach and the pressure was computed by the SIMPLE algorithm.

Numerical computations were performed on a geometry investigated experimentally by O'Malley [3]. An open circuit induced flow wind tunnel was used to provide the free-stream flow, while the injected gas was drawn from the atmosphere through a 4 cm wide slot. Boundary layer bleeds were placed at distances of 10 cm from the slot leading edge (for the mainstream) and 16 cm inside the slot (for the injectant). Numerical computations include solutions at injection ratios $B = V/U_{\text{in}} = 0.1$, 0.2, 0.5, 0.65 and 0.8. In all cases, the free-stream velocity (U_{in}) is 23 m s^{-1} and the slot width (D) is 4 cm. The flow is isothermal and both the injectant and the free-stream fluids have the density of air. The flow Reynolds number is 51 000 and the flow is fully turbulent. The only parameter varying is the inlet injection velocity.

The computational domain covered the area extending from 10 cm upstream of the slot to 60 cm downstream of the slot and a distance 52 cm above the slot. For calculations including the slot, the domain extended 16 cm into the slot. At the mainstream inlet, uniform flow was specified. No-slip boundary conditions were applied at the walls. The upper boundary was treated as an inviscid (slip) wall and standard derivative conditions were applied downstream. The slot inlet boundary condition is discussed below.

The numerical grid used was Cartesian and non-uniform, including gradual increases in density for areas of particular interest. A second-order upwind differencing scheme (BSOU), proposed by Papadakis and Bergeles [9] was implemented to improve accuracy. Numerical experiments using different grids and comparisons with results obtained using the first-order hybrid differencing scheme indicated that grid independence was achieved on a 160×160 grid, including 600 numerical points for resolving the flow inside the slot. The axial grid lines were distributed with 20 lines upstream of the slot, 20 across the slot and the remainder downstream of the slot. The resolved and unresolved slot case grids are shown in Figure 1. Convergence was assumed to be achieved when the non-dimensional residuals of mass and u, v velocities were below 0.1%. For the standard $k-\varepsilon$ with wall functions the near-wall y^+ values were about 20. For the low Reynolds number models, the grid expansion factor was adjusted to give y^+ values of less than unity.

The general transport equation used is stated below

$$\frac{\partial}{\partial x}(\rho u\Phi)+\frac{\partial}{\partial y}(\rho v\Phi)-\frac{\partial}{\partial x}\left(\Gamma_\Phi\frac{\partial\Phi}{\partial x}\right)-\frac{\partial}{\partial y}\left(\Gamma_\Phi\frac{\partial\Phi}{\partial y}\right)=S_\Phi.$$

The variables (Φ) and the respective source terms (S) of the above equation are shown in Table I for the standard k–ε model.

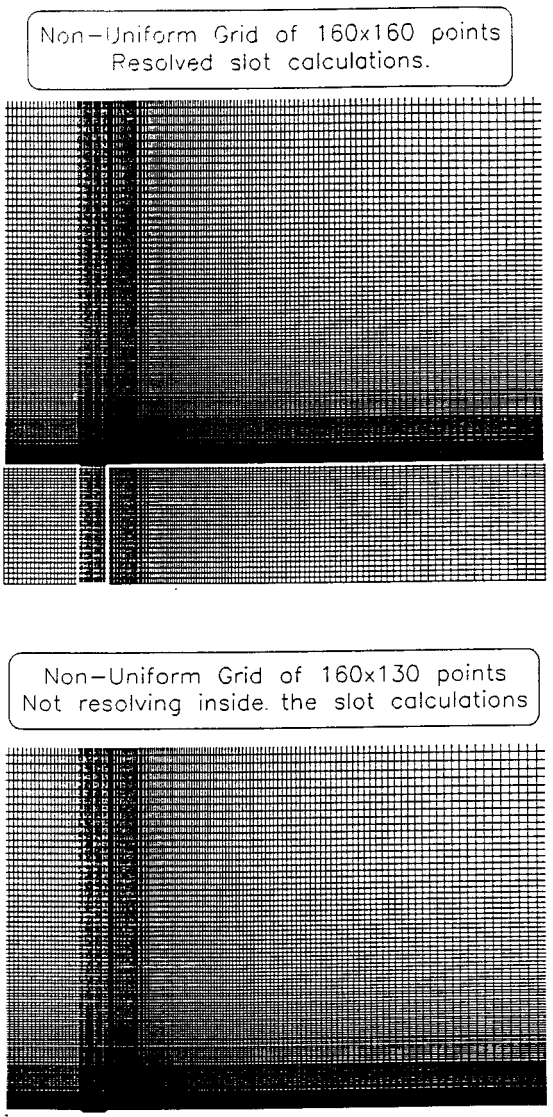

Figure 1. Numerical grids used for resolved and unresolved slot calculations.

Table I. Variables and source terms used

Φ	S_Φ
1	0
u	$-\frac{\partial p}{\partial x}+\frac{\partial}{\partial x}\left(\mu\frac{\partial u}{\partial x}\right)+\frac{\partial}{\partial y}\left(\mu\frac{\partial v}{\partial x}\right)$
v	$-\frac{\partial p}{\partial y}+\frac{\partial}{\partial x}\left(\mu\frac{\partial u}{\partial y}\right)+\frac{\partial}{\partial y}\left(\mu\frac{\partial v}{\partial y}\right)$
k	$G-\rho\varepsilon$
ε	$(C_1\varepsilon G-C_2\rho\varepsilon^2)/k$
	$G=\mu\left\{2\left[\left(\frac{\partial u}{\partial x}\right)^2+\left(\frac{\partial v}{\partial y}\right)^2\right]+\left(\frac{\partial u}{\partial y}+\frac{\partial v}{\partial x}\right)^2\right\}$

$$\mu = C_\mu \rho \frac{k^2}{\varepsilon} + \mu_1,$$

$$\Gamma_\Phi = \frac{\mu}{\sigma_\Phi},$$

where μ is the effective viscosity (the sum of the laminar and turbulent viscosities). For the k–ε turbulence model used here, the values of the constants are as follows:

$$C_1 = 1.44, \quad C_2 = 1.92, \quad C_\mu = 0.009,$$

$$\sigma_{(u,v)} = 1, \quad \sigma_k = 0.9, \quad \sigma_\varepsilon = 1.3.$$

In some computations, the curvature modification to the k–ε model, as proposed by Leschziner and Rodi [10], was applied. In this model the usual expression for turbulent viscosity is replaced by

$$v_\tau = f_\mu C_\mu \frac{k^2}{\varepsilon},$$

where

$$f_\mu = 1 + 0.57 \frac{k^2}{\varepsilon^2}\left(\frac{\partial u_s}{\partial n} + \frac{u_s}{R_c}\right)\frac{u_s}{R_c}.$$

Here R_c is the local radius of curvature of the streamline, u_s is the velocity tangential to the streamline and n is the direction normal to the streamline. For the standard model $f_\mu = 1$. Further computations used the low Reynolds number turbulence models. These involved modifications to the source terms in the k and ε equations and required solutions in the near-wall region rather than of wall function boundary conditions.

3. RESULTS

3.1. Mainstream flow predictions with the standard k–ε model

In this paper the results at high and low blowing ratios will be presented; i.e. for the cases $B = 0.8$ and 0.1. However, a graph showing the recirculation length as a function of the blowing ratio includes numerical values at intermediate ratios. As seen in Figure 2 there is a linear relationship of the form $X/D = 13.1B + 0.3$ between the reattachment length and the respective injection ratio. This is confirmed both from numerical results and experimental data,

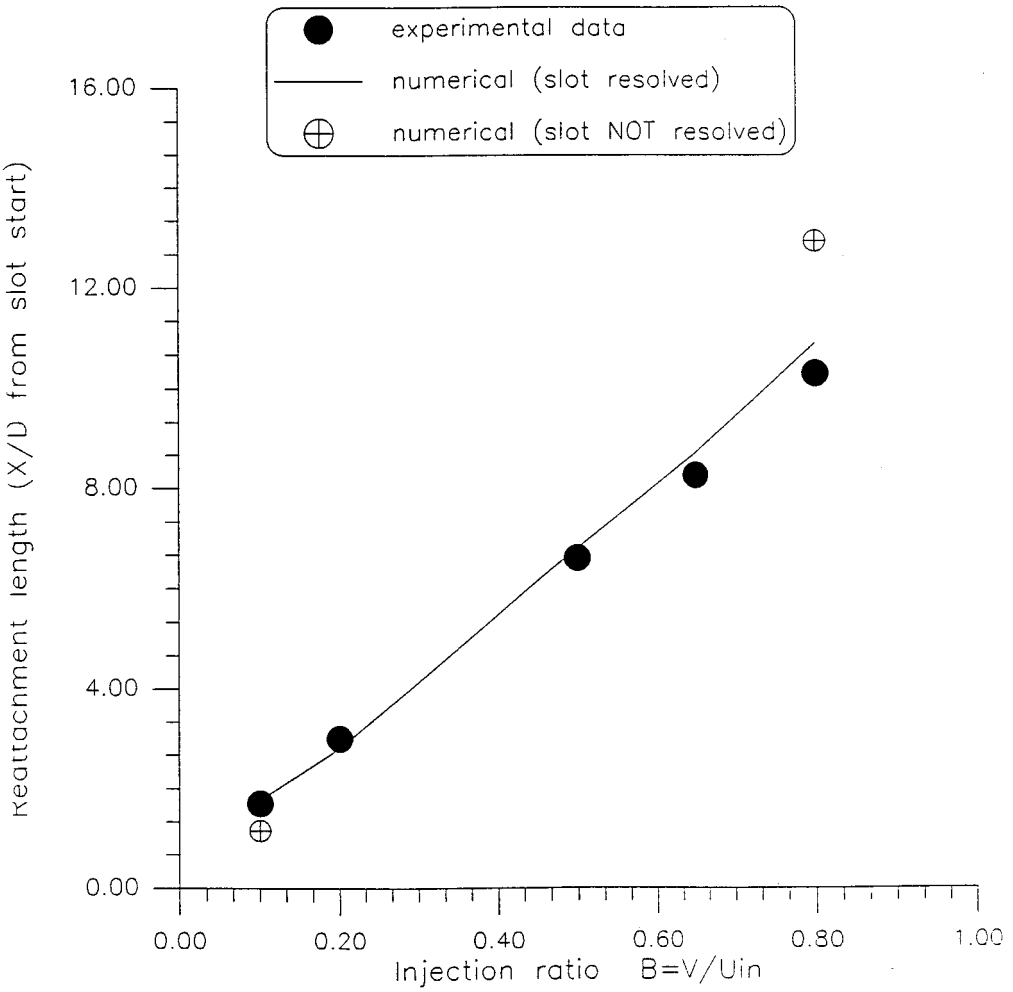

Figure 2. Reattachment length for different blowing ratios.

which are in close agreement with each other. As this ratio increases, the recirculation region grows as expected, to reach a length of $10.3D$ at the highest injection flux. In this graph, two values were obtained assuming a uniform velocity profile at the jet exit (slot not resolved). Even if the relationship in question is linear, it seems to follow a higher slope leading away from experimental data. This was a first indication that further investigation of the injectant behaviour inside the slot was needed. A detailed analysis will follow in the next section.

It is interesting to observe the streamlines of the flow for the two blowing cases. For the low injection ratio ($B = 0.1$), where the theoretical model of Fitt *et al.* [1] applies, the so-called 'lid effect' can be seen. The dividing streamline (marked on Figure 3) is tangential to the wall and the injectant escapes from a region near the slot's trailing edge. For the high injection ratio, the 'lid effect' disappears and the injection takes place throughout the slot. It should be stated that for the high blowing ratio, where the mixing process and penetration are more severe, close agreement with the experimental data is obtained. The recirculation region for the $B = 0.8$ case can be clearly seen in Figure 4, where the reattachment point is at about $10.3D$.

As seen from the wall pressure distributions graphs in Figure 5, there is a similar pattern between numerical results and experimental data for different blowing ratios. In the recirculation region, there is a region in which the pressure coefficient remains constant. The pressure then rises gradually to reach its free-stream value downstream. The velocity profiles in the x-direction (Figure 6) reveal that, within the separated region, vorticity decreases with distance. The change in the slope of the velocity is sharp initially and smoother further away from the slot. Thus, a constant vorticity region can be assumed in, approximately, the latter half of the recirculation region, particularly for high injection ratios. Observing Figures 5 and 6 closely, it can be said that the separated region divides itself into two parts: the first is characterised by constant pressure and large variations in vorticity; the second is characterised by velocity profiles that indicate constant vorticity with increasing pressure. In the case of the high injection ratio ($B = 0.8$), the constant pressure region ($1 < X/D < 6$) and the constant

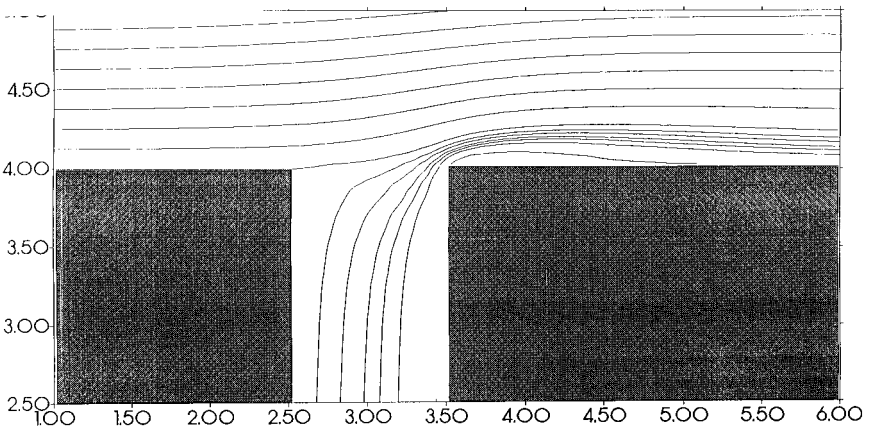

Figure 3. Streamlines for $B = V/U_{\text{in}} = 0.1$.

vorticity region ($6 < X/D < 10$) are more clearly seen. In the same case, the maximum velocity reaches a value of $1.4U_{in}$ (Figure 6). This is to be expected since from continuity, the external flow has to accelerate to overcome the obstacle created by the secondary fluid and the separated flow. From Bernoulli's equation, this leads to a wall pressure coefficient of -0.9, approximately. As the maximum velocity decreases with distance from the slot and approaches the free-stream velocity, U_{in}, the pressure rises as expected. This effect appears at the low injection ratio as well (velocity profiles shown in Figure 7), but is less apparent than in the high injection ratio. Numerically, it can be said that although good agreement is achieved with the experimental data generally, the $k-\varepsilon$ model is unable to predict accurately the velocity distribution in the region of the near-wall recirculation. In the pressure coefficient graphs, good matching is achieved at the wall both before and after the slot. In the slot region, the numerical pattern follows a similar shape with the experimental data but overpredicts the peak at the slot leading edge that occurs due to the injection.

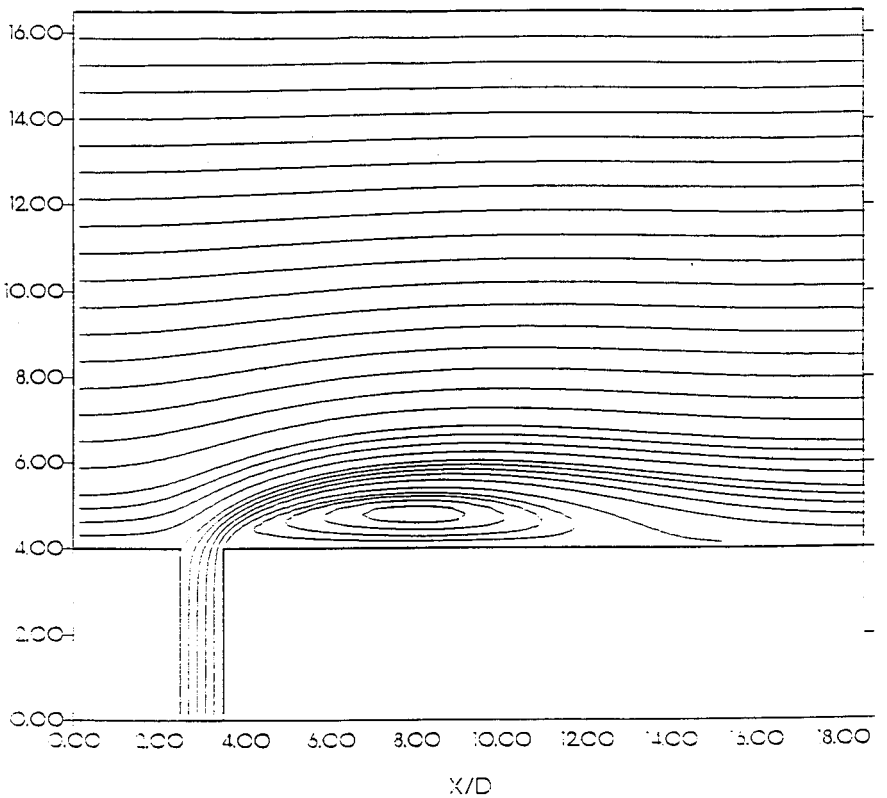

Figure 4. Streamlines for $B = V/U_{in} = 0.8$.

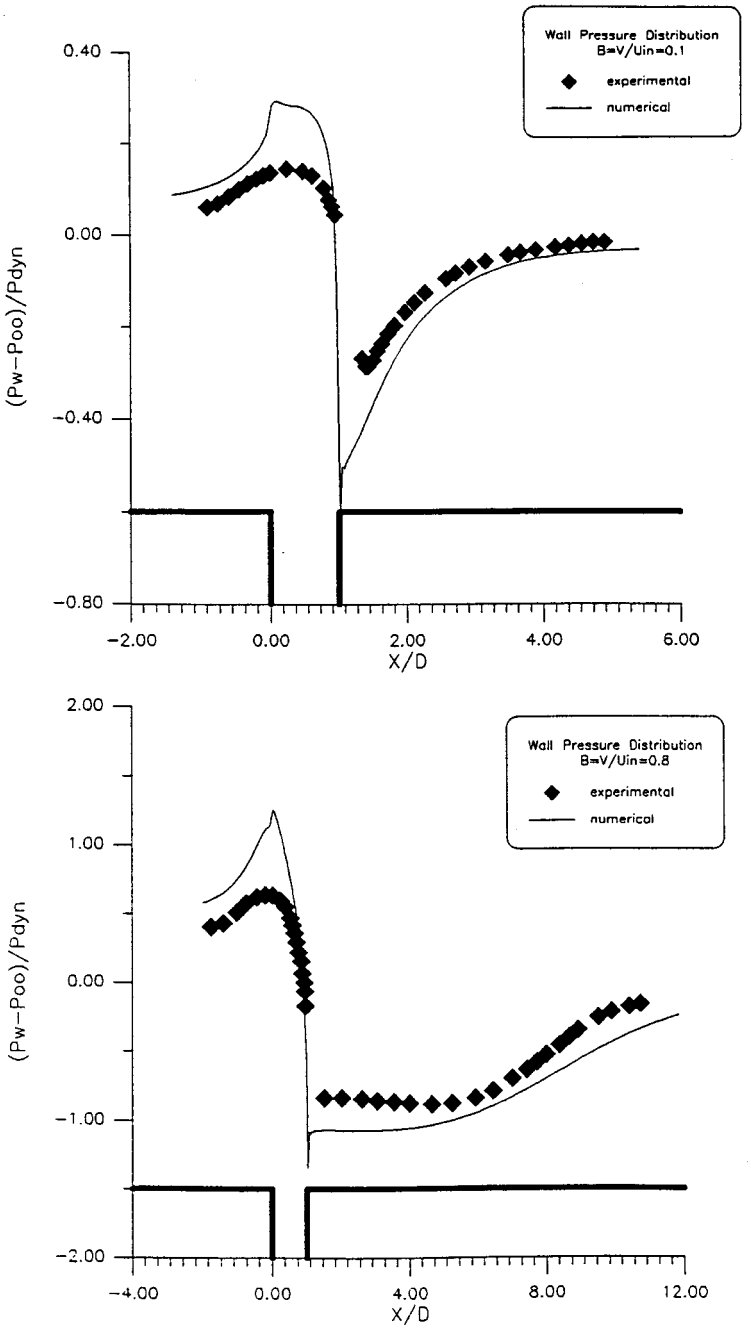

Figure 5. Wall pressure distributions for $B = 0.1$ and 0.8.

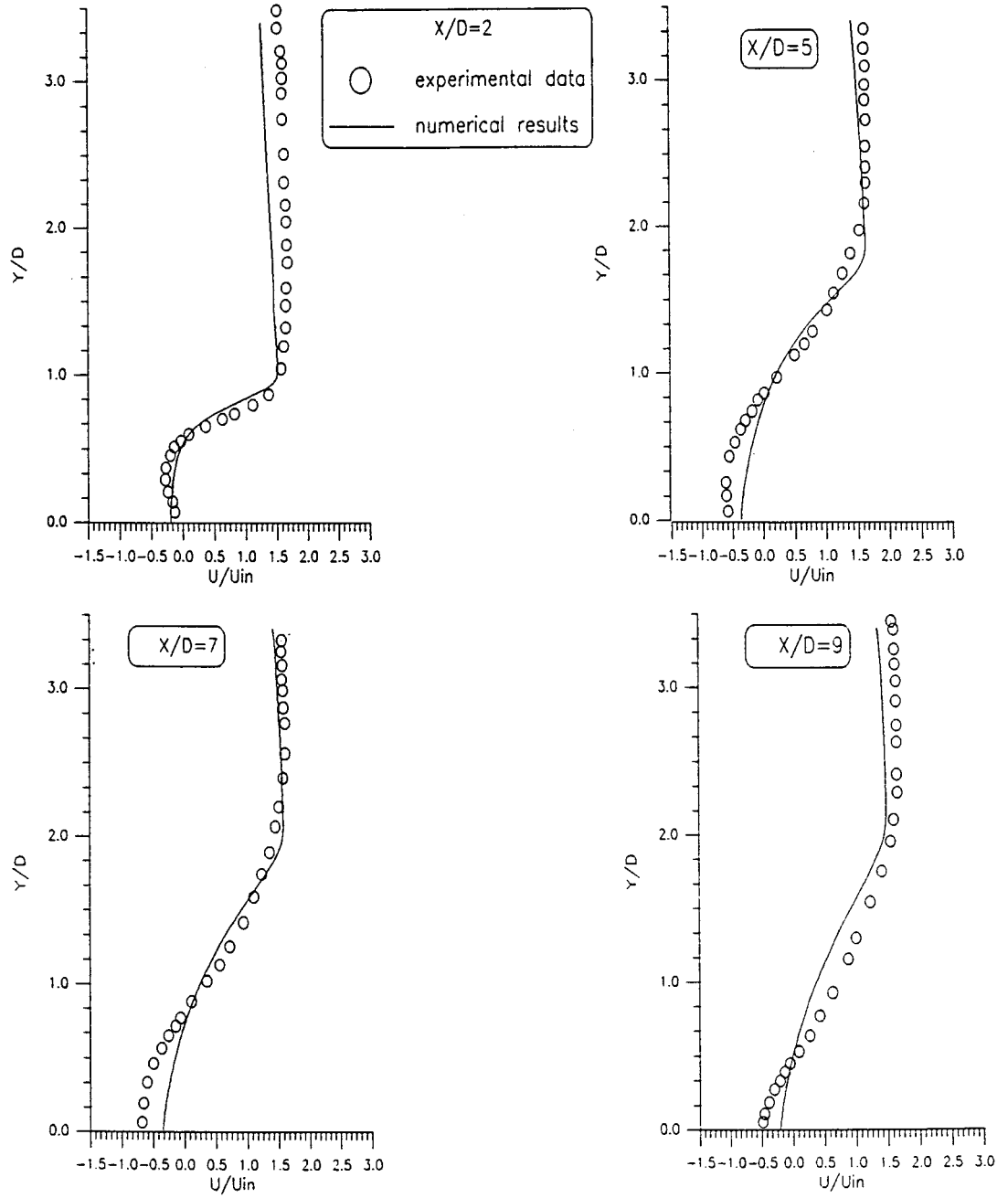

Figure 6. U velocity profiles for $B = 0.8$.

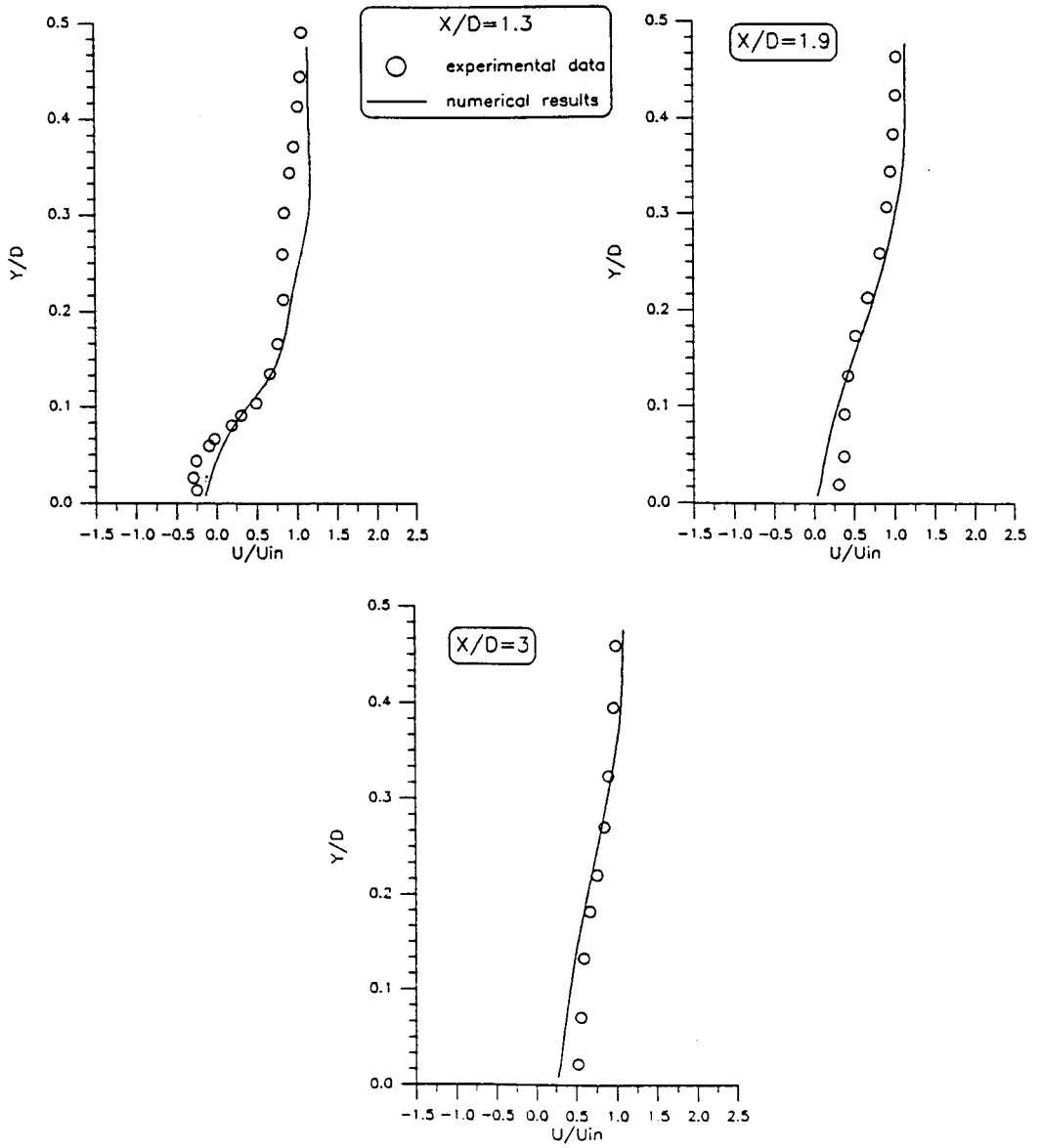

Figure 7. U velocity profiles for $B = 0.1$.

3.2. Sensitivity to turbulence model assumptions

An attempt has been made to improve the near-wall computations of the flow field using a different turbulence model than the standard $k-\varepsilon$ with wall functions. Initially, the curvature modification to the $k-\varepsilon$ model, proposed by Leschziner and Rodi [10], and then two low Reynolds number turbulence models were used, namely those of Lam and Bremhorst [11] and Launder and Sharma [12]. The curvature modification introduces an expression for the model parameter C_μ that depends on streamline curvature. Another curvature modification model (not examined here) was suggested by Prassas *et al.* [13] improving, in some test cases, the numerical results. The comparison of the suitability of the models was based on the low blowing ratio case ($B = 0.1$) and the respective velocity profiles, since convergence was hard to achieve for the high blowing ratios. From the profiles in Figure 8, it can be seen that the low Reynolds number turbulence models offer no obvious improvement to the standard $k-\varepsilon$ model. Near the wall, their behaviour is not consistent, since there is a tendency to better approach the experimental data in some positions but not in others. Moving away from the wall, the models tend to the $k-\varepsilon$ prediction as expected from the theory. The curvature modification of the standard model, on the other hand, seems to produce a slight improvement in the recirculation region, while being identical with the $k-\varepsilon$ curve at all other positions. This conclusion is consistent with there being greater dissipation at areas of high curvature (e.g. recirculation). Outside this area, the streamlines smoothen and the modification has no influence at all on the standard model, as illustrated by the graphs. Thus, we conclude that for a fully turbulent boundary layer on a film cooling geometry, the standard $k-\varepsilon$ model is the most reliable (with the possible addition of the curvature modification) and the easiest to implement. The low Reynolds number models used here have proved their value in the past showing excellent agreement with experimental data in many cases. However, in the geometry examined here, there is no substantial contribution towards the improvement of the $k-\varepsilon$ model, also presenting some difficulty in convergence. A possible reason for this failure is that these models are calibrated, and extensively used for 'single flow cases', i.e. there is only one, primary flow.

A slot cooling flow field involves a mixing process and penetration from a secondary fluid (injectant) that may not be compatible with a low Reynolds number approach. The curvature modification, however, is not affected by this peculiarity since it just takes into account the curvature of the streamline at a point in the flow. Similar findings were reported by Alvarez *et al.* [14] when comparing a Reynolds stress model with the standard $k-\varepsilon$ model on a slot geometry. The two turbulence models yielded essentially the same results with slight deviations.

3.3. Flow behaviour inside the slot

Profiles of the velocities tangential to the slot axis were obtained for different positions inside the slot, for the two blowing ratios. As seen in Figures 9 and 10, three profiles are examined at distances of $1.5D$, $2.9D$ and $4D$, where the slot's total height is $4D$. Although there is a similar behaviour up to a distance of about three quarters of the slot, the high and low injection case produce a notably different exit velocity profile. At $Y/D = 1.5$, the flow is similar to that of the developing pipe flow. In the next position ($Y/D = 2.9$), the effect of the

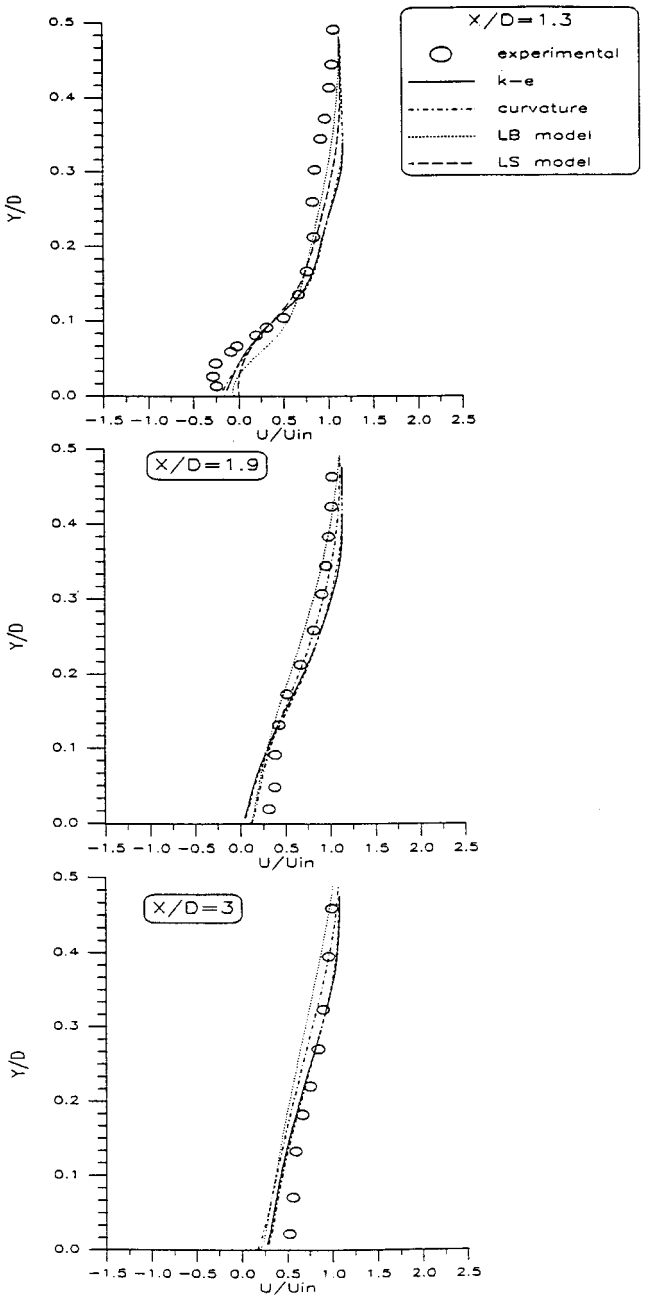

Figure 8. U velocity profiles predicted for $B = 0.1$ with different turbulence models.

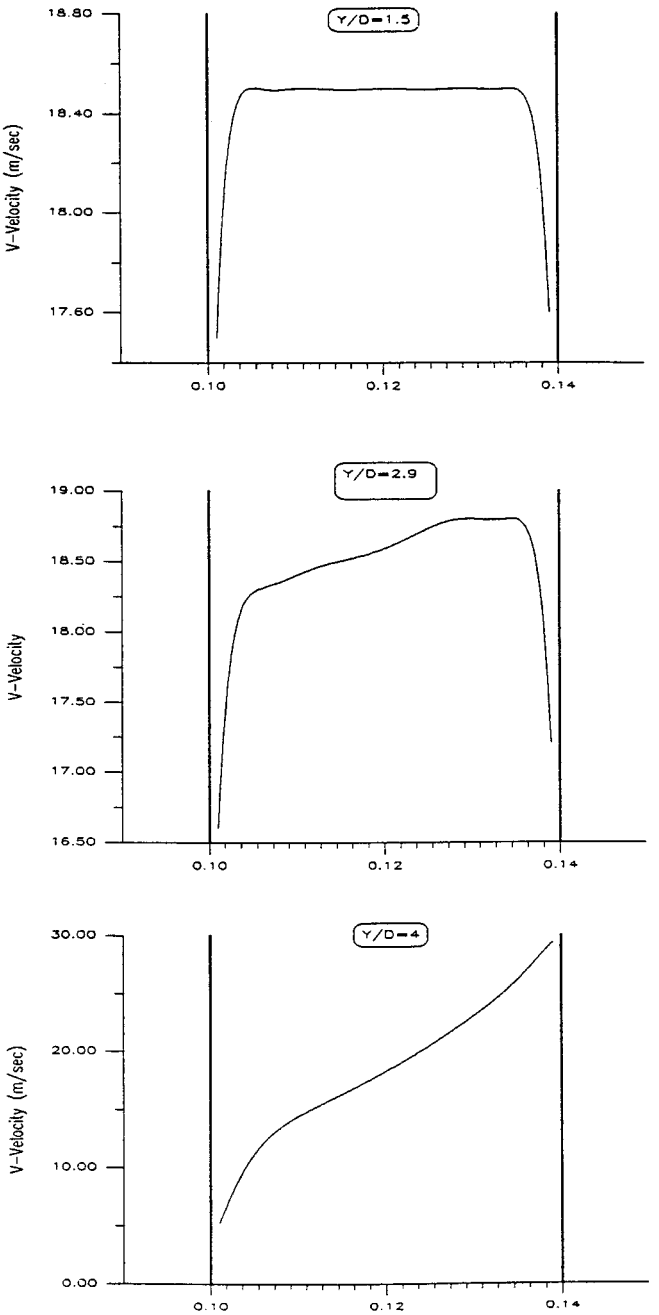

Figure 9. Development of V velocity for $B = 0.8$ inside the slot of total height $4D$.

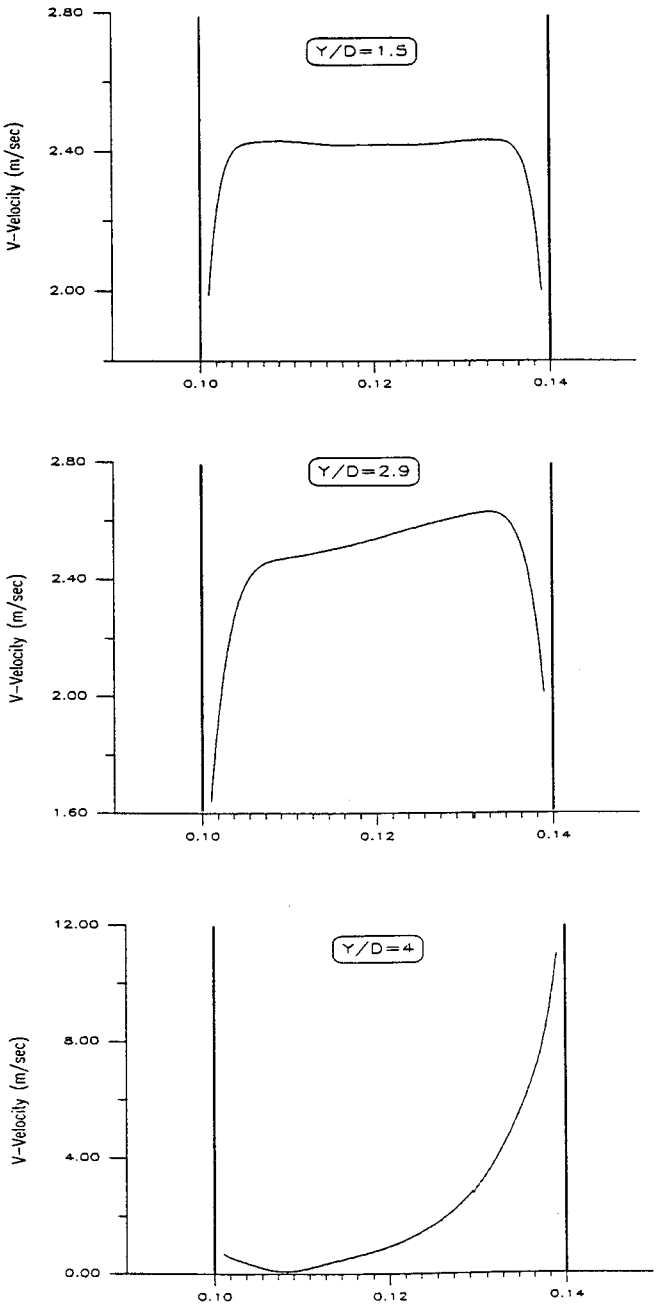

Figure 10. Development of V velocity for $B = 0.1$ inside the slot of total height $4D$.

mainstream flow is evident and pressure effects lead velocities to increase near the slot's rear wall. At the exit, both cases show high velocities near the downstream wall. In the first half of the slot, i.e. near the upstream wall, there is no similarity between the velocity patterns of the two blowing cases. It is apparent that this 'first half' behaviour is dependent on the injection ratio; furthermore, if the injection ratio was even lower, a 'recirculation bubble' would appear at the front edge of the slot. As far as total pressure is concerned, the difference in the pattern

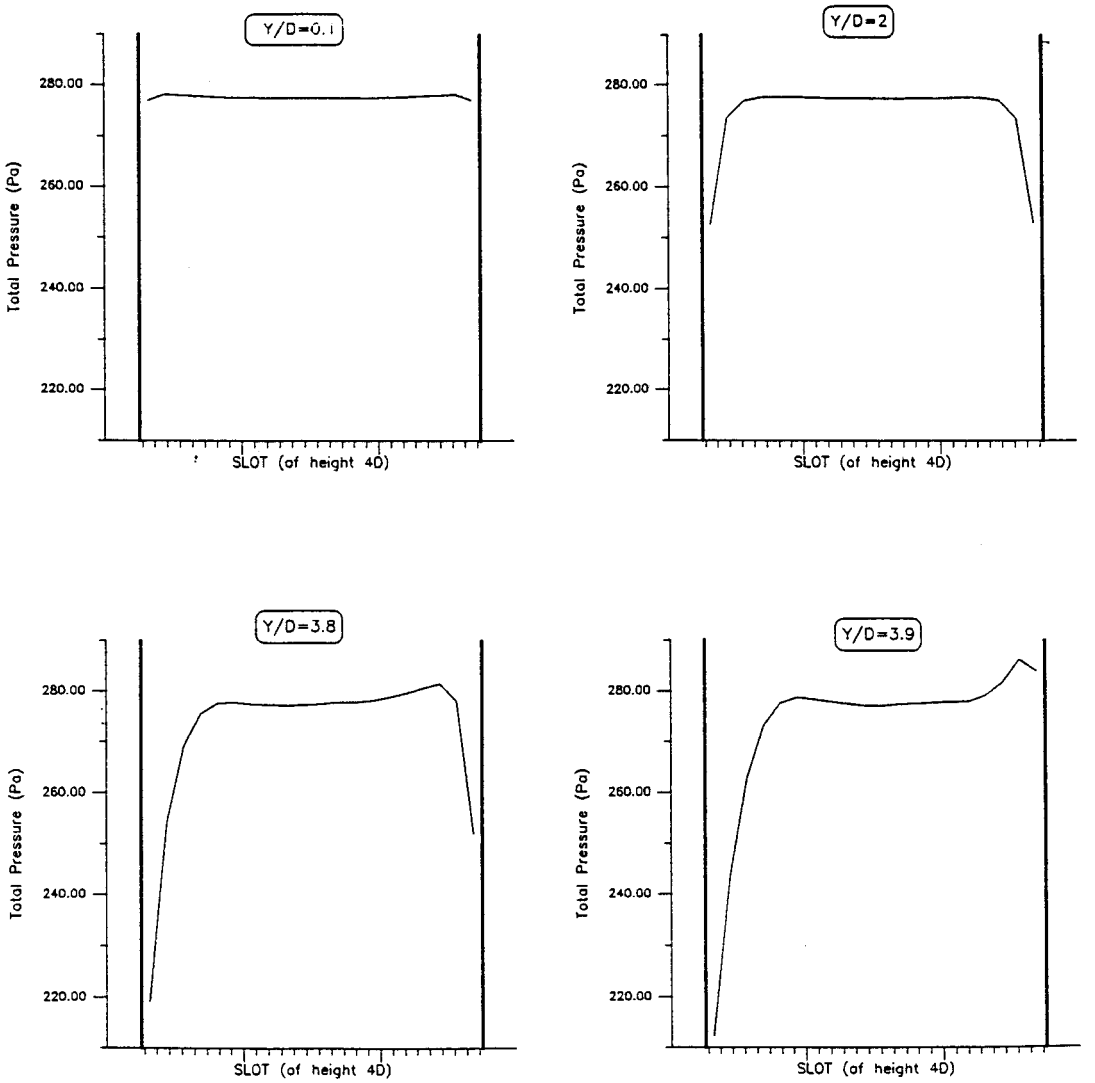

Figure 11. Total pressure variation for $B = 0.8$ inside the slot of height $4D$.

of the two cases is more severe. Figures 11 and 12 demonstrate the stagnation pressure development inside the slot at four positions, namely those of $0.1D$, $2D$, $3.8D$ and $3.9D$. Again, up to $2D$ there is a similar behaviour; energy losses are apparent near the walls due to friction. At $3.8D$ there is no significant change for the high blowing ratio, while a completely different behaviour is observed for the low ratio; total pressure is increasing up to the point of its

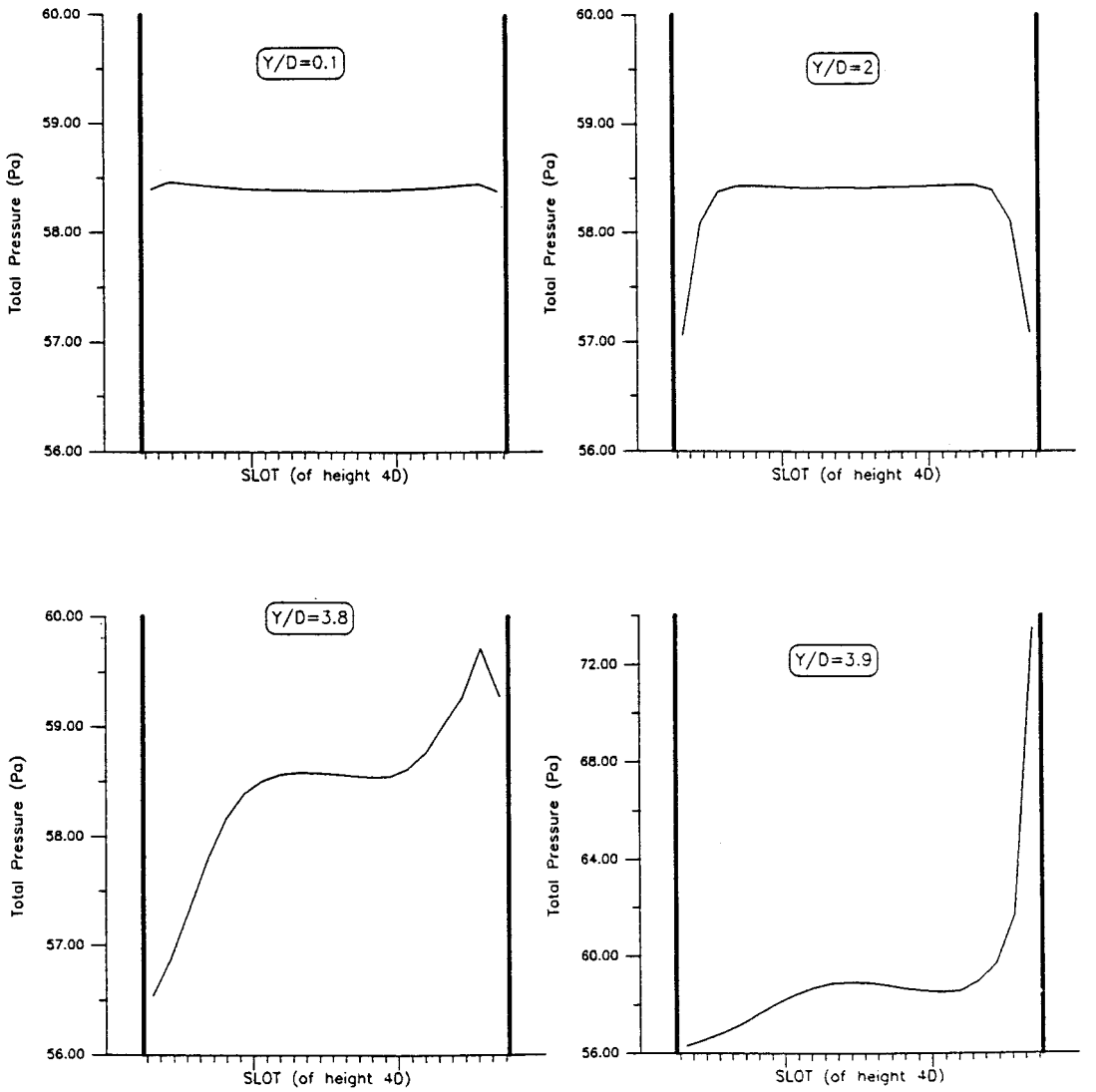

Figure 12. Total pressure variation for $B = 0.1$ inside the slot of total height $4D$.

average value, remains constant for a distance and then increases again. This can be interpreted as the effect of the main flow becoming significant. This is also demonstrated by the abrupt change in pattern between $Y = 3.8D$ and $3.9D$. In the last profile, i.e. at $Y = 3.9D$, the stagnation pressure is high only close to the rear slot wall. Taking into account the static pressure distribution at the slot exit, we can better explain the 'lid effect'. Since the static pressure is small for the slot exit area (Figure 5) and the total pressure is high only at the rear edge of the slot, it can be expected that the injectant velocity is much higher at the rear edge. Furthermore, this effect is due to the recovery of free-stream pressure over the shape of the emerging injectant; the high velocity at the rear of the slot comes about due to the very low static pressure at the rear plus a viscous accelerating effect at low blowing rate as described above. Thus, most of the injectant escapes from a small area near the jet's rear wall, as shown from the streamlines in Figure 3. In Figure 12, the total pressure can only increase above the mid passage value owing to the viscous effects of the free-stream, i.e. as the free-stream is travelling much faster than the injectant at the low blowing rate, it accelerates the injectant by viscous effects as it leaves the rear of the slot. This is not seen for the high blowing rate case because the total pressure of the injectant is close to that of the mainstream; furthermore, the total pressure profile for the $B = 0.8$ case is almost uniform for all positions inside the slot. This last remark is crucial since an attempt has been made to produce a better boundary condition at the slot exit. Observing the velocity and the total pressure profile at the exit for the high blowing ratio, it is clear that a boundary condition based on total pressure would yield more accurate results than one based on velocity. At the higher blowing rates, the viscous effects are small and hence the total pressure should be constant and provide a better boundary condition.

3.4. Slot exit boundary conditions

From the above discussion it is obvious that the commonly used assumption of a uniform velocity profile at the slot exit is an inappropriate boundary condition. It leads to a significant loss of accuracy, particularly at the region near the slot, and lacks a physical basis. This can be clearly seen from Figure 13, where velocity profiles are plotted for the resolved-slot case and the unresolved-slot case (using the constant velocity boundary condition). In all cases the pattern of the resolved slot results is in close agreement with the experimental data; on the other hand, assuming a uniform velocity at the jet exit yields results that have a tendency to move away from both the experimental data and the resolved slot computations. Thus, taking into account the recirculation length predictions and the velocity profiles shown above, it can be said that this boundary condition is inappropriate for cases where the near-slot behaviour (e.g. recirculation region) is of great importance.

Observing the behaviour of the stagnation pressure inside the slot for high blowing ratios, it is clear that this physical quantity could offer a much better approximation to the resolved case. Total pressure variations are negligible in most parts of the slot area; energy losses are expected near the jet's walls due to friction and are not significant. Thus, a boundary condition based on total pressure was attempted for the jet exit to test its suitability compared with the one previously used (constant velocity profile). The slot

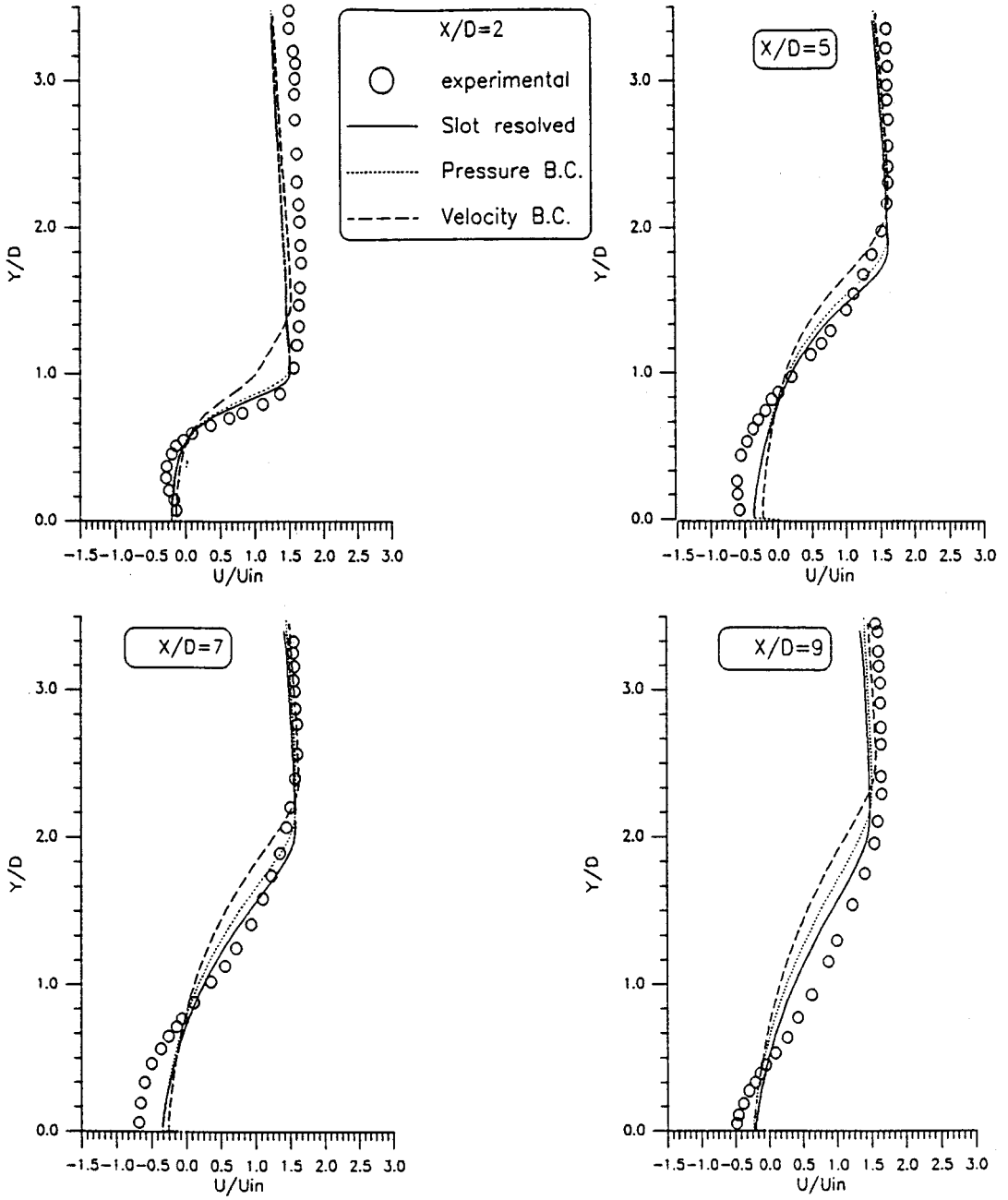

Figure 13. Comparison of the pressure and velocity boundary conditions for $B = 0.8$.

boundary condition imposed assumed uniform total pressure with the total pressure level being adjusted to give the required injection flow rate. Further assumptions involved the velocity being tangential to the slot ($U = 0$) and the streamwise pressures gradient being zero ($\partial p/\partial y = 0$). During each iteration of the solution scheme, the uniform total pressure is adjusted so that the mass flow through the slot equals the required value, and Bernoulli's equation is satisfied. That is, at the slot exit,

$$P_{\text{tot}} = p + \frac{1}{2}\rho v^2,$$

$$M_{\text{in}} = \int_0^D \rho v \, \mathrm{d}x.$$

The superiority of this boundary condition as opposed to the flat velocity profile at the slot exit is demonstrated in Figure 13. In all positions the total pressure boundary condition is much closer to the resolved case results (and the experimental data) being identical in some positions. The CPU time needed for convergence is almost identical for the two boundary conditions. Thus, we can conclude that for blowing ratios greater than $B = V/U_{\text{in}} = 0.5$ approximately, the method used above provides improved accuracy in all aspects of the near-slot modelling. This boundary condition aims to better simulate the flow field where the flow inside the normal jet cannot be efficiently resolved. This maybe the case for a turbine blade's multiple slots or holes, designed for effective film cooling.

4. CONCLUSIONS

The aerodynamics of a two-dimensional slot cooling geometry have been studied numerically and reasonably good agreement with experimental data was achieved. Two types of models were used for the simulation of turbulence: The well-established two-equation k–ε model and three low Reynolds number models were implemented into the code producing no significant differences. The behaviour of the injection fluid inside the slot was examined with particular emphasis at the slot exit. The 'lid effect' was observed for the low injection ratio and explained physically. The shape of the exit velocity profile was found to vary for the high ($B = 0.8$) and the low ($B = 0.1$) injection and was by no means uniform. However, the total pressure profile at the slot exit was essentially uniform for the high injection ratio. Thus, a boundary condition based on total pressure was developed and compared with the usual uniform velocity assumption at the jet exit. The pressure-type boundary condition yielded numerical results in good agreement with the resolved slot case and therefore with the experimental data. The velocity boundary condition produced less accurate results, particularly in the region near the slot. This pressure boundary condition for a jet exit in cross-flow can be easily modified for a three-dimensional geometry. Finally, the length of the recirculation bubble seems to be linearly correlated to the blowing ratio.

APPENDIX A. NOMENCLATURE

U_{in}	free-stream inlet velocity
V	injection inlet velocity
B	velocity injection ratio (V/U_{in})
D	slot width
P_{w}	wall static pressure
P_{∞}	free-stream static pressure
P_{dyn}	dynamic head ($1/2\rho U_{\text{in}}^2$)

REFERENCES

1. A.D. Fitt, J.R. Ockendon and T.V. Jones, 'Aerodynamics of slot-film cooling: theory and experiment', *J. Fluid Mech.*, **160** (1985).
2. A.D. Fitt and P. Wilmott, 'Slot-film cooling—the effect of separation angle', *Acta Mech.*, **103** (1994).
3. K. O'Malley, 'Theoretical aspects of film cooling', *D.Phil. Thesis*, University of Oxford, 1984.
4. G. Bergeles, A.D. Gossman and B.E. Launder, 'The near-field character of a jet discharged normal to the mainstream', *J. Heat Transf.*, **98c** (1976).
5. G. Bergeles, A.D. Gossman and B.E. Launder, 'The near-field character of a jet discharged through a wall at 30 degrees to a mainstream', *AIAA J.*, **15** (1977).
6. J. Andreopoulos, 'Measurements on a pipe flow issuing perpendicular into a cross stream', *J. Fluids Eng.*, **104** (1983).
7. D.E. Metzger, H.J. Carper and L.R. Swank, 'Heat transfer film cooling near nontangential injection slots', *ASME J. Eng. Power*, **90a** (1968).
8. A.J.H. Teekaram, C.J.P. Forth and T.V. Jones, 'Film cooling in the presence of mainstream pressure gradients', *ASME J. Turbomach.*, **113** (1991).
9. G. Papadakis and G. Bergeles, 'A locally modified second order upwind for convection terms discretization', *Int. J. Numer. Methods Heat Fluid Flow*, **5** (1995).
10. M.A. Leschziner and W. Rodi, 'Calculation of annular and twin parallel jets using various discretization schemes and turbulence-model variations', *ASME J. Fluids Eng.*, **103** (1981).
11. C.K.G. Lam and K.A. Bremhorst, 'Modified form of the $k-\varepsilon$ model for predicting wall turbulence', *J. Fluids Eng.*, **103** (1981).
12. B.E. Launder and B.I. Sharma, 'Application of the energy-dissapation model of turbulence to the calculation of flow near a spinning disc', *Lett. Heat Mass Transf.*, **1** (1974).
13. I. Prassas, G. Papadakis and G. Bergeles, 'Numerical simulation of particle dispersion in a vertical round sudden expansion flow', *Numer. Methods Lam. Turbul. Flow*, **8** (1993).
14. J. Alvarez, W.P. Jones and R. Seoud, 'Predictions of momentum and scalar fields in a jet in crossflow using first and second order turbulence closures', *AGARD CP-534 Computational and Experimental Assessment of Jets in Cross Flow*, 1993.

